ACS APPLIED MATERIALS & INTERFACES

Research Article

www.acsami.org

# Tunable Electrical Memory Characteristics Using Polyimide:Polycyclic Aromatic Compound Blends on Flexible Substrates

An-Dih Yu,[†,‡] Tadanori Kurosawa,[†,§] Ying-Hsuan Chou,[†,‡] Koutarou Aoyagi,[§] Yu Shoji,[§] Tomoya Higashihara,[§] Mitsuru Ueda,*[,§] Cheng-Liang Liu,*[,⊥] and Wen-Chang Chen*[,‡]

[‡]Department of Chemical Engineering, National Taiwan University, Taipei, 10617 Taiwan

[§]Department of Organic and Polymeric Materials, Tokyo Institute of Technology, 2-12-1 Ookayama, Meguro-ku, Tokyo 152-8552, Japan

[⊥]Department of Chemical and Materials Engineering, National Central University, Taoyuan, 32001 Taiwan

Supporting Information

**ABSTRACT:** Resistance switching memory devices with the configuration of poly(ethylene naphthalate)(PEN)/Al/polyimide (PI) blend/Al are reported. The active layers of the PI blend films were prepared from different compositions of poly[4,4′-diamino-4″-methyltriphenylamine-hexafluoroisopropylidenediphthalimide] (**PI(AMTPA)**) and polycyclic aromatic compounds (coronene or *N*,*N*-bis[4-(2-octyldodecyloxy)-phenyl]-3,4,9,10-perylenetetracarboxylic diimide (**PDI-DO**)). The additives of large π-conjugated polycyclic compounds can stabilize the charge transfer complex induced by the applied electric field. Thus, the memory device characteristic changes from the volatile to nonvolatile behavior of flash and write-once-read-many times (WORM) as the additive contents increase in both blend systems. The main differences between these two blend systems are the threshold voltage values and the additive content to change the memory behavior. Due to the stronger accepting ability and higher electron affinity of **PDI-DO** than those of coronene, the **PI(AMTPA)**:**PDI-DO** blend based memory devices show a smaller threshold voltage and change the memory behavior in a smaller additive content. Besides, the memory devices fabricated on a flexible PEN substrate exhibit an excellent durability upon the bending conditions. These tunable memory performances of the developed PI/polycyclic aromatic compound blends are advantageous for future advanced memory device applications.

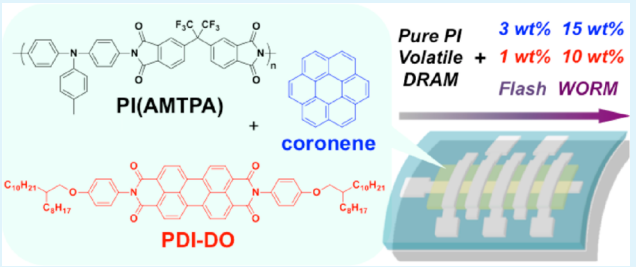


**KEYWORDS:** *memory, polymer blend, polyimides, polycyclic aromatic compounds, flexible devices*

## INTRODUCTION

The field of flexible electronics has the potential revolution for lightweight and inexpensive electronics if the memory components can be integrated on physically flexible substrate in a reliable way. The simple structure in resistor-type memory device, which generally consists of a thin film of active layer sandwiched between two metal contacts, contributes to its compatibility with future flexible electronics.[1−5] Data storage that relies on the difference in resistances with applied voltage can permanently or temporarily distinguish the digital "0" and "1" states of memory bits by probing with a low reading voltage. Organic materials have the advantages over the inorganic counterparts because of the inherent flexibility of the compound, versatility of the chemical structures, low cost, and simplified processing.[1−5] The integration of resistor memories with other flexible devices using organic polymeric materials may enable the realization of future computing recoding medium. Among the reported materials for resistor memories,[1−11] polymer blend materials have the advantages than others because of their easy and diverse modulation of the host polymers and guest additives to control the resulted memory characteristics.[1,4,12] Typical guest additives can be embedded within polymers such as metal nanoparticles (NPs),[13−16] graphitic carbon-based nanomaterials (fullerenes,[17−28] nanotubes,[29,30] and graphene[31−34]), organic small molecules,[35−37] and polymer molecules.[38] The underlying mechanisms of resistance switching in these blend materials range from the traps randomly distributed throughout the entire region of host matrix to electric field induced charge transfer from donor to acceptor between the moieties. The polymers act as an electrically functional host or just a supporting matrix, whereas the guest additives have an interaction with polymers or within themselves. The concentration and distribution of the additives in the blend system play an important role in the reversibility or volatility of electronic resistance observed in the thin film state under external electrical stress.

Received: February 21, 2013
Accepted: May 7, 2013
Published: May 7, 2013

 © 2013 American Chemical Society  dx.doi.org/10.1021/am4006594 | ACS Appl. Mater. Interfaces 2013, 5, 4921−4929

Functional polyimides (PIs) exhibiting charge transfer behavior between electron donor and acceptor moieties could have the electrical bistability under an applied electric field.[9−11,39−42] Our previous work showed that the incorporation of large resonance structures (perylene, pyrene, or naphthalene) into PIs through the copolymer approaches[9−11] manifested the stability of charge transfer complex. However, a simple strategy on homogeneous polymer blend can take advantage of exhibiting macroscopically uniform physical properties without complex synthetic procedure for making copolymers but with similar functionalities. Therefore, it would be of interest of using PIs as functional hosts blended with the polycyclic aromatic compounds as guest additives to tune the memory characteristics through the donor−acceptor charge transfer.

Here we report on the resistance switching memory characteristics based on the blend materials of poly[4,4′-diamino-4″-methyltriphenylamine-hexafluoroisopropylidene-diphthalimide] (**PI(AMTPA)**) and polycyclic aromatic compounds, as shown in Figure 1. Two solution-processable

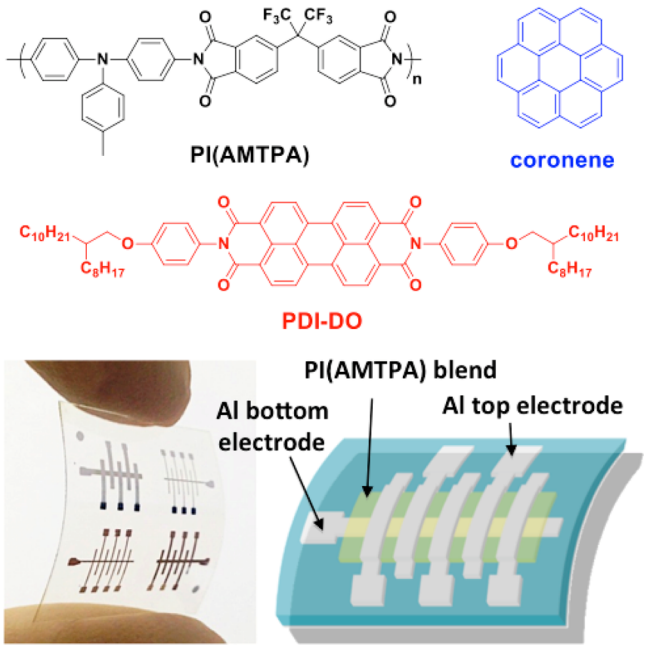


**Figure 1.** Schematic diagram of the memory device configuration and the chemical structures of PI matrix and polycyclic aromatic compound additives.

polycyclic aromatic compounds with different energy levels, coronene and *N,N*-bis[4-(2-octyldodecyloxy)phenyl]-3,4,9,10-perylenetetracarboxylic diimide (**PDI-DO**), were applied as additives blended with **PI(AMTPA)** as the memory storage materials. The flexible resistor memory devices with the configuration of the poly(ethylene naphthalate) (PEN)/Al/PIs blend/Al were fabricated and characterized. The device performance as function of bending radius and the repeated bending test was studied to ensure the potential memory devices.

## EXPERIMENTAL SECTION

**Materials.** All commercially available reagents or anhydrous solvents obtained from suppliers were used without further purification unless otherwise noted. **PI(AMTPA)** host matrix was prepared according to the our reported procedure.[9,10] Anhydrous chloroform was purchased from Aldrich (USA). Coronene was directly purchased from Tokyo Chemical Industry (TCI) Co., Ltd. (Japan). The synthesis of precursory amine compound (1-amino-4-(2-octyldocecyloxy)benzene; **3**) for **PDI-DO** is described in the Supporting Information.

**Synthesis of PDI-DO.** The synthesis and characterization of **PDI-DO** are shown in Scheme S1 and Figures S1−S3 of the Supporting Information. The mixture of compound **3** (0.591 g, 1.52 mmol), 3,4,9,10-perylenetetracarboxylic dianhydride (0.199 g, 0.508 mmol), and imidazole (3.17 g) was heated at 180 °C for 3 h under argon atmosphere. Then, the reaction mixture was poured into methanol to precipitate the crude product. The product was purified by Soxhlet extraction using methanol and $CHCl_3$. After evaporating $CHCl_3$, the product was further purified by silica gel column chromatography using $CH_2Cl_2$ as an eluent, followed by freeze-drying from its absolute benzene solution, to afford **PDI-DO** as red solid (0.462 g, 80%). $^1$H NMR (300 MHz, $CDCl_3$, $\delta$, ppm, 25 °C): 8.57 (d, $J$ = 7.8 Hz, 4H, aromatic proton), 8.32 (d, $J$ = 8.4 Hz, 4H, aromatic proton), 7.30 (d, $J$ = 9.0 Hz, 4H, aromatic proton), 7.06 (d, $J$ = 9.0 Hz, 4H, aromatic proton), 3.90 (d, $J$ = 5.7 Hz, 4H, O−$CH_2$—), 1.88−1.75 (m, 2H, O−$CH_2$—$CH$), 1.55−1.23 (m, 64H, —$CH_2$—), 0.96−0.85 (m, 12H, —$CH_3$). $^{13}$C NMR (75 MHz, $CDCl_3$, $\delta$, ppm, 25 °C): 163.56, 159.70, 134.38, 131.44, 129.64, 129.38, 127.12, 126.17, 123.55, 123.15, 115.41, 71.23, 38.14, 32.09−27.04 (14 carbons), 22.85 (2 carbons), 14.29 (2 carbons). IR (KBr), $\nu$ ($cm^{-1}$): 2924 (alkyl C−H), 1707, 1666 (C═O stretching), 1360 (C−N stretching). MS (MALDI-TOF) $m/z$ [M +H$^+$]: Calcd for $C_{76}H_{98}N_2O_6$, 1134.74. Found, 1135.09. Anal. Calcd for $C_{76}H_{98}N_2O_6$: C, 80.38; H, 8.70; N, 2.47. Found (%): C, 80.29; H, 8.69; N, 2.45.

**Characterization.** $^1$H and $^{13}$C NMR spectra were recorded on a Bruker DPX (300 MHz) in chloroform-*d* calibrated to tetramethylsilane (TMS) as an internal standard ($\delta_H$ 0.00). FT-IR spectra were measured on a Horiba FT-720 spectrometer. Matrix-assisted laser desorption ionization time-of-flight (MALDI-TOF) mass spectrum was recorded on a Shimadzu AXMACFR mass spectrometer. The spectrometer was equipped with a nitrogen laser (337 nm) and with pulsed ion extraction. The operation was performed at an accelerating potential of 20 kV by linear-positive ion mode. Dithranol was used as a matrix. Mass values were calibrated by the three-point method with insulin plus H+ at $m/z$ 5734.62, insulin $\beta$ plus H+ at $m/z$ 3497.96, and $\alpha$-cyanohydroxycinnamic acid dimer plus H+ at $m/z$ 379.35. Elemental analysis was carried out on a YANACO CHN corder MT-6. UV−vis absorption spectral data were measured with Hitachi U-4100 spectrophotometer. Fluorescence spectra were collected by a Fluorolog-3 spectrofluorometer (Jobin Yvon). Thin film measurements were collected by spin-coating onto untreated quartz substrate. The thickness of polymer film was determined with a Microfigure Measuring Instrument (Surfcorder ET3000, Kosaka Laboratory Ltd.). The morphology of that active layer **PI(AMTPA)**:coronene or **PDI-DO** blend films was examined by atomic force microscopy (AFM; Digital Instruments, Santa Barbara, CA) in tapping mode.

**Device Fabrication and Characterization.** PEN substrate was first precleaned by an ultrasonic cleaning process with water, isopropanol, and acetone successively for 15 min each. Al bottom electrode lines with a thickness of 30 nm were deposited via a thermal evaporation at a pressure of $10^{-5}$ Torr with a depositing rate of 1 Å $s^{-1}$. Four mg $mL^{-1}$ of **PI(AMTPA)** in tetrahydrofuran (THF) or chloroform were mixed with calculated numbers (0−15%) of coronene or **PDI-DO** additives and sonicated for 30 min to form homogeneous solutions. Then, the well-mixed solutions were filtered through 0.22 $\mu$m pore size of PTFE membrane syringe filter, spin-coated onto the bottom Al electrode/PEN substrate at 1000 rpm for 60 s and baked at 100 °C on a hot plate in $N_2$-filled glovebox. The thickness of the PI blend active layer was determined to be 40 nm. The top electrode lines were aligned perpendicular to the bottom lines, leading to cross-point arrays of memory cells with active joint area of 0.2 × 0.2, 0.4 × 0.4, and 0.6 × 0.6 $mm^2$, respectively. All the electrical characteristics of the fabricated flexible memory devices were measured by a Keithley 4200-SCS semiconductor parameter analyzer (with low noise preamplifier) using a probe station at room

temperature in a $N_2$-filled glovebox. The bottom electrode was grounded during all the electrical measurement with a swept step of 0.05 V.

## RESULTS AND DISCUSSION

**Characterization of PI Blend Materials.** The **PI(AMTPA)** and coronene (or **PDI-DO**) blend are conveniently dispersed in common organic solvents with a brief sonication treatment. The clear dispersion remains stable without any trace of precipitates at ambient conditions, indicating the good miscibility between **PI(AMTPA)** and coronene (or **PDI-DO**). Thin films spin-coated from a solution of **PI(AMTPA)**:coronene (or **PDI-DO**) show a smooth morphological surface (Figure S4 in the Supporting Information) investigated by AFM. No surface phase-separated aggregation is observed among the guest additives in the **PI(AMTPA)** matrix.

Figure 2 and Figure S5 (Supporting Information) show the absorption spectra of different contents of coronene or **PDI-DO** in the **PI(AMTPA)** solution and thin film, respectively. The absorption peak at 302 nm and adjoining pronounced shoulder from **PI(AMTPA)** are assigned to the delocalized $\pi-\pi^*$ transitions of the triphenylamine moieties. The intensities of the absorbance peak from pure coronene or **PDI-DO** are basically increased with the additive content. Panels a and b in Figure 3 show the photoluminescence (PL) spectra of **PI(AMTPA)**:coronene and **PI(AMTPA)**:**PDI-DO** blend thin film, respectively, at the excitation wavelength of 329 nm. The fluorescence is more quenched especially in the **PI(AMTPA)**:**PDI-DO** blend (82% decease in PL intensity based on 10% **PDI-DO**) than that of **PI(AMTPA)**:coronene (56% decease in PL intensity based on 15% corenene), clearly indicating efficient charge transfer of the former. Thus, stable charge separated state within the donor/acceptor system of **PI(AMTPA)**:**PDI-DO** could obviously happen. It explains the possible guest additive−host matrix interaction associated with the charge-transfer-related switching mechanism.

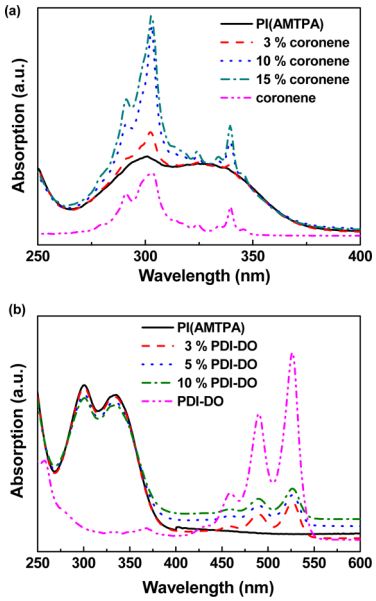


**Figure 2.** Absorption spectra of (a) **PI(AMTPA)**:coronene and (b) **PI(AMTPA)**:**PDI-DO** blend solution.

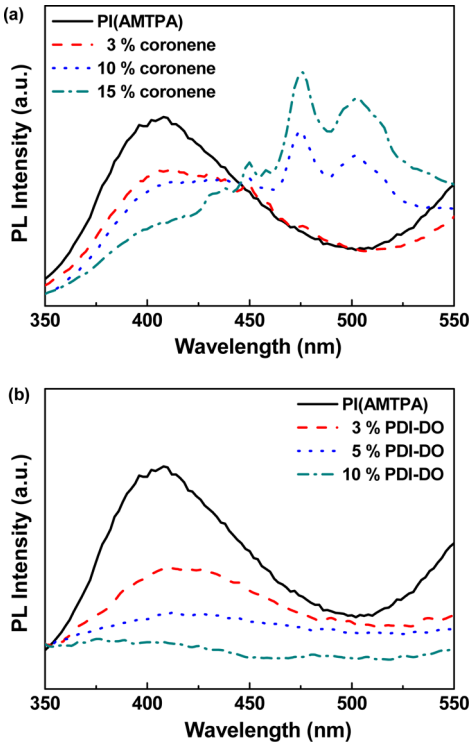


**Figure 3.** Photoluminescence spectra of (a) **PI(AMTPA)**:coronene and (b) **PI(AMTPA)**:**PDI-DO** blend thin films.

**Memory Characteristics.** The memory device is constructed using the PI blend film as the sandwiched layer in the arrays of three-layer cross-point device with Al as both top and bottom electrodes (Figure 1). All the fabrications and measurements are conducted in the chemically inert condition without any atmospheric oxygen to facilitate the charge injection from electrode. Instead of relying on an additional diode or transistor as the selective device, our device uses the logical organization on the square of single row (bit-line; utilized as bottom electrode). Thus, several columns (word-line; utilized as top electrode) are obtained in the resistive switches to break the sneak current paths from passing through the nonselected cells. The memory device is organized into the memory cells and each stores one binary bit. Our pattern significantly simplifies the device fabrication process and enables the selected device cells to be operated correctly. Therefore, we can directly understand the electrical characteristics of PIs blend film from the simple cross-point array of memory cells without any possibilities on misreading. Figures 4 and 5 show the current density−voltage ($J-V$) curves in semilog plot of the memory devices on PEN flexible substrates fabricated from **PI(AMTPA)**:coronene and **PDI-DO** blends, respectively (linear $J-V$ curves in Figure S6 of *Supporting Information*). Similar to our previous report,[9,10] the device based on **PI(AMTPA)** (without additives) exhibits a volatile dynamic random access memory (DRAM) characteristic observed by subsequent voltage sweeps (data not shown here). In the device with 3% of coronene or **PDI-DO** with respect to the **PI(AMTPA)**, the bipolar-type hysteresis behavior is observed as indicated by the dc voltage sweep of Figures 4b and 5b. The voltage is cyclically swept from 0 to −4 V (or −3.5 V), −4 V (or −3.5 V) to 0 V, 0 to 3 V, and 3 to 0 V. While steadily increasing the voltage in the negative direction, the current jumps abruptly at a critical voltage that implies an expected change of resistance from the high resistance state (HRS) to low resistance state (LRS). The HRS to LRS


dx.doi.org/10.1021/am4006594 | ACS Appl. Mater. Interfaces 2013, 5, 4921−4929

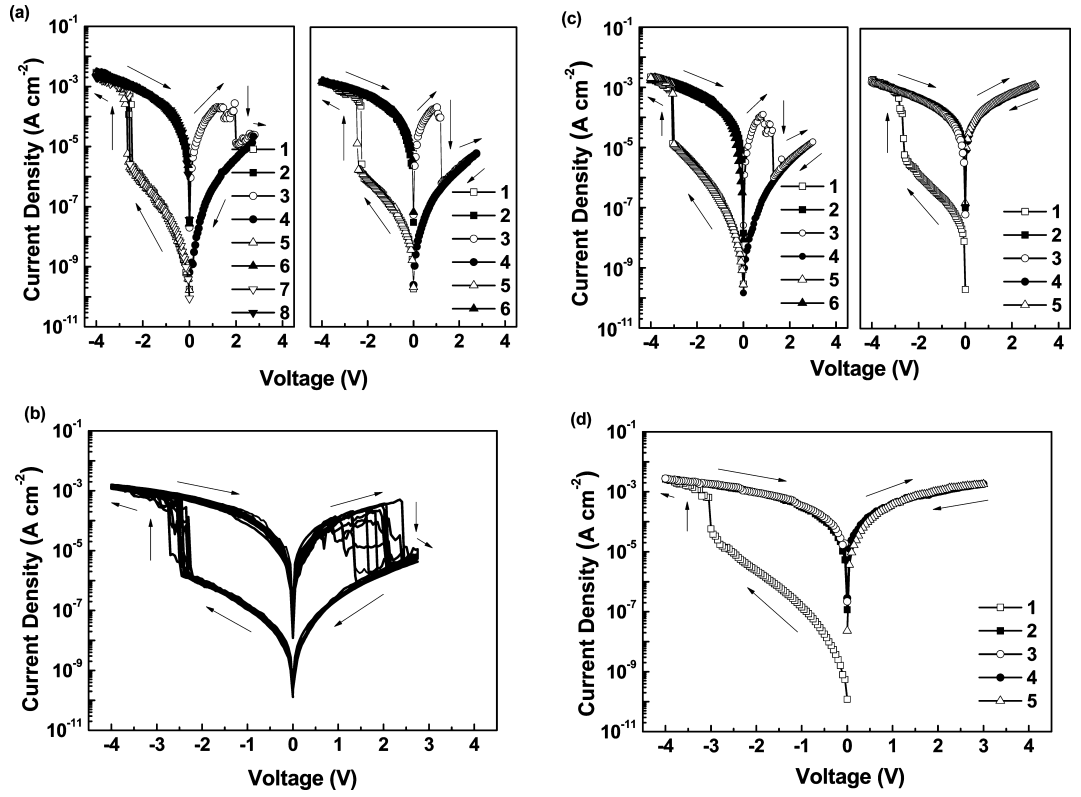


**Figure 4.** Current density−voltage ($J$−$V$) of the memory devices using **PI(AMTPA)** blended with (a) 1, (b) 3, (c) 10, and (d) 15% coronene, respectively.

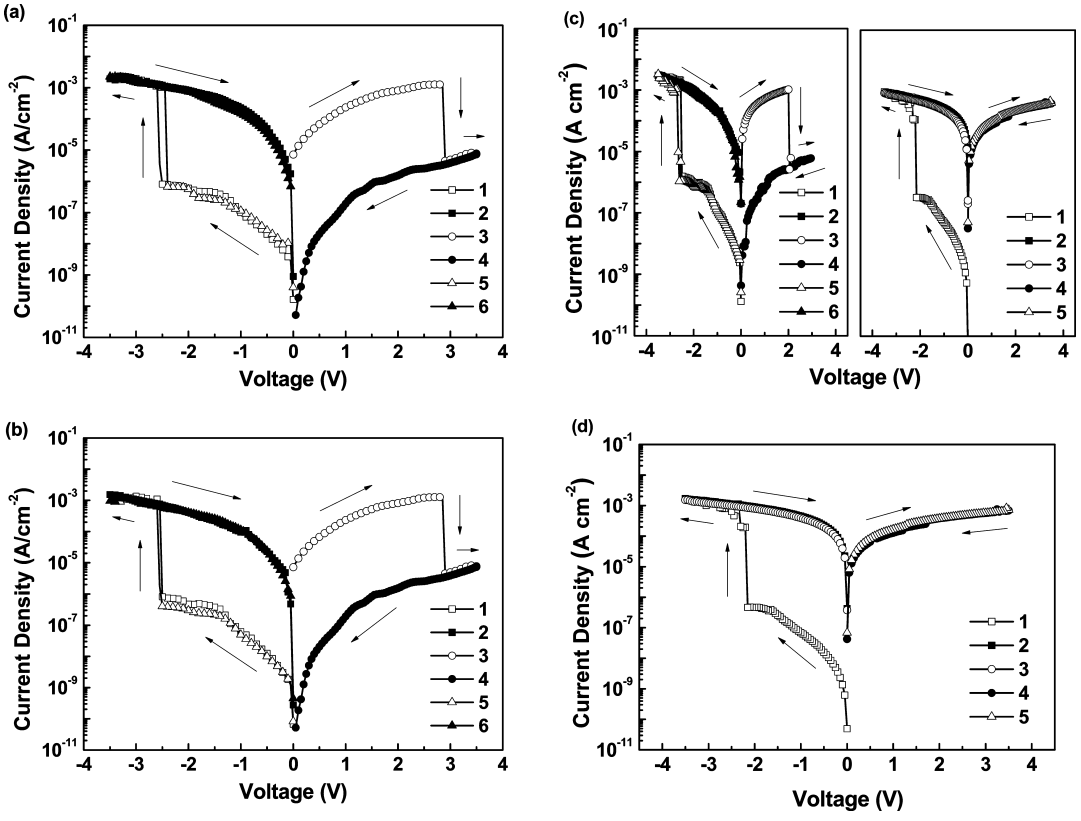


**Figure 5.** Current density−voltage ($J$−$V$) of the memory devices using **PI(AMTPA)** blended with (a) 1, (b) 3, (c) 5, and (d) 10% **PDI-DO**, respectively.


dx.doi.org/10.1021/am4006594 | *ACS Appl. Mater. Interfaces* 2013, 5, 4921−4929

switching is called the "SET" or "writing" process and the corresponding threshold voltage is defined as $V_{th}$(SET). When the voltage is swept to the opposite direction from 0 to 3 V, the device holds the LRS and then recovers to the origin HRS at the voltage range of ~1.3−2.4 V. The LRS to HRS switching is the "RESET" or "erasing" process and the corresponding switching voltage is defined as $V_{th}$(RESET). The LRS/HRS can be retained in the following "reading" process (from −4 to 0 V or 3 to 0 V). LRS is commonly used as ON state while HRS as OFF state. Bipolar switching is defined in these blend devices if they are realized in SET and RESET process by applying alternating voltage polarity. A high ON/OFF current ratio larger than $10^4$ is achieved at 1 V, which may provide a low misreading rate during the reading operation. In addition, the current density in LRS could be preserved for more than two weeks without any electrical treatment. The device switches between HRS and LRS steadily and both the HRS and LRS are nonvolatile, suggesting a flash-type memory. A low SET/RESET power of ~1 mW cm$^{-2}$ is measured in the PEN/Al/PI blend/Al devices. The symmetric switching −-$V$ curves are possibly ascribed to the similar work function of bottom/top Al electrodes. Here, 1% coronene memory device shows the transition in performance between volatile[9] (Figure 4(a) left) and nonvolatile flash (Figure 4a, right) although the 1% **PDI-DO** device reveals flash memory only (Figure 5a). When the high loading content of additive (15% coronene or 10% **PDI-DO**) is added, the current traces still exhibit the bistable phenomena during the first dual voltage scan (Figures 4d and 5d). The device demonstrates an HRS with a current density scale on the order of $1 \times 10^{-10}$ to $1 \times 10^{-6}$ A cm$^{-2}$, and current density increases dramatically to the order to $1 \times 10^{-4}$ to $1 \times 10^{-3}$ A cm$^{-2}$ as the applied voltage reaches $V_{th}$(SET). However, the LRS in the device is remained and cannot be recovered by applying a high voltage in either polarity. Such inerasable and irreversible data storage can be employed for the application of the nonvolatile write-once-read-many-times (WORM) memory element. At the moderate loading contents of the additives in the blend (10% coronene or 5% **PDI-DO**), the devices statistically perform 80% WORM as well as 20% flash behavior out of 30 studied cells. It clearly shows that the introduction of coronene or **PDI-DO** additives dramatically affects the electrical performance on both volatility and erasing ability.

The retention performance of 3% coronene or 1% **PDI-DO** in **PI(AMTPA)** is shown in Figure 6. The device is read at −1 V for formed ON or OFF state and the current is monitored every 90 s. There is no significant change in the current density at both states during the test duration for at least $10^4$ s and the device still remains a large sensing margin, indicating good retention capability. Furthermore, Figure 7 (or Figure S7 in the Supporting Information) shows the cyclic voltage stress at −3.5 V (or 3 V) for writing, 3 V for erasing and −1 V for reading from 1 to 200 (50) cycles for **PI(AMTPA)**:3% coronene (or **PDI-DO**) blend device. The devices exhibit a highly stable characteristic with well-resolved states in terms of operating repeated write-read-erase-read (WRER) sequence test. In all cases, the LRS can be restored to the HRS successfully. The highly controllable resistance modulation of the blend device implies that the conducting pathway is repeatedly formed and ruptured under alternative bias polarity.

For flexible electronics application, the device bending durability is becoming significant. Therefore, we conduct a primary study on flexible memories based on our **PI(AMTPA)** blend materials using transparent and flexible PEN substrate instead of typical used ITO or Si/SiO$_2$ substrate. The **PI(AMTPA)**:coronene or **PDI-DO** devices show excellent mechanical properties on the bending test as a function of bending condition (from flat to bending radius of 30, 20, 10,

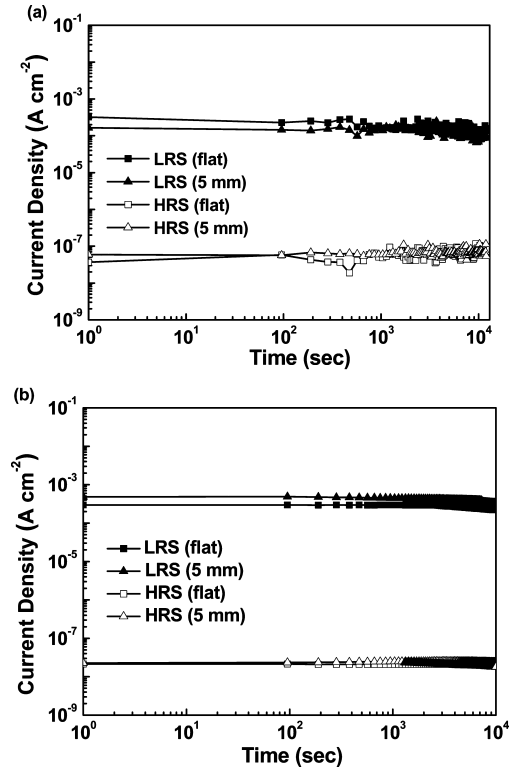


**Figure 6.** Retention time test of the flexible memory devices under the flat and bending conditions using the blends of (a) **PI(AMTPA)**:3% coronene and (b) **PI(AMTPA)**:3% **PDI-DO**.

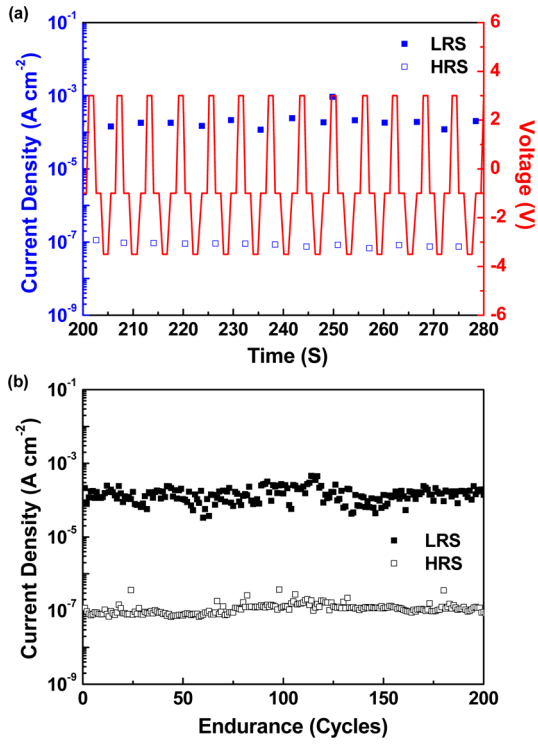


**Figure 7.** (a) WRER cycles and (b) endurance of the memory device using the blend of **PI(AMTPA)**:3% coronene.


dx.doi.org/10.1021/am4006594 | ACS Appl. Mater. Interfaces 2013, 5, 4921−4929

and 5 mm). Nonvolatile flash-type devices fabricated from **PI(AMTPA)**:3% coronene or **PDI-DO** (Figure 8) and

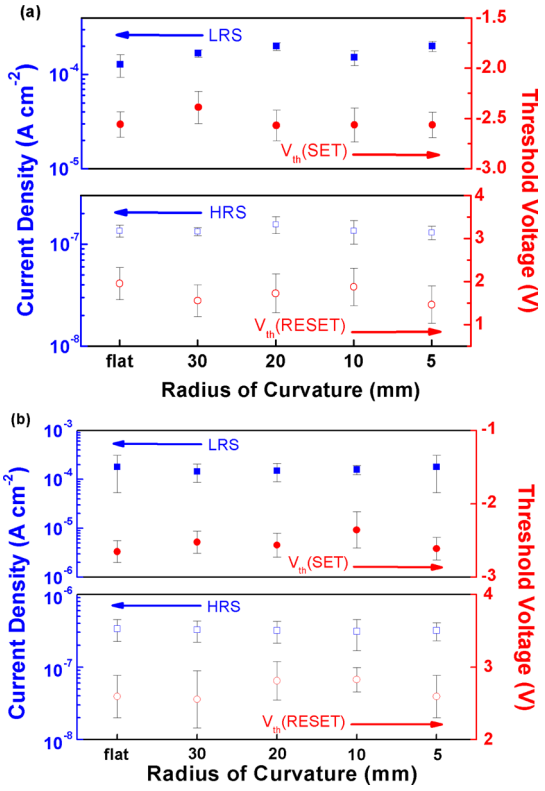


**Figure 8.** Variation in current density and threshold voltages of the flexible blend memory devices under different bending condition using the blends of (a) **PI(AMTPA)**:3% coronene and (b) **PI(AMTPA)**:3% **PDI-DO**.

WORM-type devices from **PI(AMTPA)**:15% coronene or 10% **PDI-DO** (Figure S8 in the Supporting Information) are used for the flexibility test. In each condition, standard deviations calculated from 10 data of critical performing parameters (including $V_{th}$(SET) or $V_{th}$(RESET) and current density at LRS or HRS) are statically analyzed. Regardless of the bending condition, no significant alternation in the current density value at LRS or HRS is observed. Narrow distributions of those parameters emphasize that the switching behavior is quite stable for realistic use even under severely compressed condition. After the substrates are repeatedly bent to for semicircular shape, data retention is measured (Figure 6). Within the time frame of $1 \times 10^4$ s, the initial state and the state after writing do not show any significant degradation at room temperature. This indicates that the device has an excellent data retention ability and mechanical robustness. In addition to flexibility, the reliability of the flexible memories is investigated by measuring electrical characteristics (a couple of writing/erasing process was performed to collect the current responses) on operation of repeating up to 1000 bending cycles. The key electrical parameters plotted in Figure S9 in the *Supporting Information*, including current density at LRS/HRS, are not significantly degraded. The current density remains nearly constant value of $\sim 1 \times 10^{-4}$ and $1 \times 10^{-7}$ A cm$^{-2}$ for LRS and HRS, respectively. All these device characteristics on PEN substrates are in a narrow distribution, which demonstrate a reliable operation in a flexible form. Therefore, our PI blend-based resistor memory features with low-voltage constrain and simple fabrications are more competing for flexible electronic applications.

**Operation Mechanism.** According to external voltage stimuli, the studied memory cells show bistable LRS/HRS switching levels. To elucidate the resistor switching phenomena, various switching mechanisms have been proposed for resistor memories using organic polymer-based materials such as filamentary conduction, electric-ield-induced charge transfer interaction, and charge trapping/detrapping process.[2,4] The native $Al_2O_x$ layer would not be involved in the obtained bistable switching characteristics because all the fabrications and measurements were done inside the $N_2$-filled glovebox (inert atmosphere). For the conductive filaments, metal migration/diffusion into active thin film results in the formation of highly conductance of metallic filament paths. Here, low LRS current density (much lower than current compliance) and the lack of necessary forming process or device breakdown in our PI blend devices are speculated to exclude the metal filament mechanism. To explain the current flow due to an applied voltage, carrier transport mechanisms were analyzed through isothermal $J-V$ correction. The related physical models have been described by follows: space-charge-limited conduction (SCLC; including ohmic conduction ($J \approx V$) and child's law region ($J \approx V^2$)),[43,44] and Poole-Frenkel (P−F) emission ($\ln(J/V) \approx V^{1/2}$).[2,45] There are two different regions in the HRS. At the low voltage region of HRS in PIs blend (3% coronene or **PDI-DO**) flash memory, standard ohmic conduction model is dominated. It suggests a linear relationship of $J-V$ curve, whereas in the high voltage region, the current density shows the square dependence of the voltage that confirms the child's mode (Figure 9). The SCLC can determine the charge carrier injection and hopping through the PIs blend thin films in HRS.

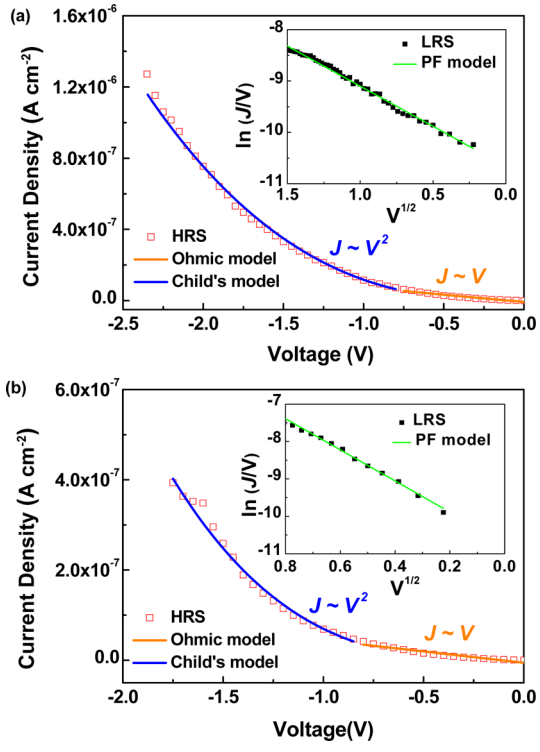


**Figure 9.** Experimental and fitted $J-V$ characteristics of the flexible blend memory devices using the blends of (a) **PI(AMTPA)**:3% coronene and (b) **PI(AMTPA)**:3%**PDI-DO**.


dx.doi.org/10.1021/am4006594 | *ACS Appl. Mater. Interfaces* 2013, 5, 4921−4929

When the voltage exceeds $V_{th}$(SET), the current density increases exponentially with an obvious switching transition. After that, the charge injection/conduction in LRS (inset of Figure 9) is well fitted to the conventional P−F emission as the ln $(J/V)$ is proportional to $V^{1/2}$. The P−F emission is associated with the lowering of electrically charged barrier in the bulk active layer when an external field exists. Current flow by the P−F emission occurs only when the numerous generated charges have sufficient energy to overcome the barrier of charge transfer state. However, similar change of conduction models between the HRS/LRS were reported in previous work.[9,10,17,22] We observed that the charge transfer from the highest occupied molecular orbital (HOMO) of the donors to the lowest unoccupied molecular orbital (LUMO) of the acceptors dominated the switching conduction in PI memory cells. Besides, the HRS/LRS transition of the WORM-type PI blend (15% coronene or 10% **PDI-DO**) can also obey the appropriate theoretical model (Figure S10 in the Supporting Information).

The mechanism of pure **PI(AMTPA)** can be explained from electric-field-induced charge transfer between triphenylamine donor and phthalimide acceptor.[9−11] With the increase in the applied bias, the excitation of triphenylamine donor promotes the intra- or intermolecular charge transfer state which gives rise to a decrease in resistance. Thus, the positive and negative charges are separately located on donor and acceptor, respectively. Once the guest additives are doped inside the **PI(AMTPA)** matrix, the geometrical $\pi$-conjugated interaction and relative frontier orbitals (Figure 10) determine the

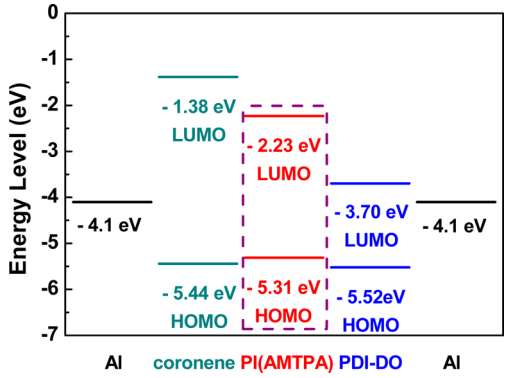


**Figure 10.** Relative energy levels of Al, **PI(AMTPA)**, coronene, and **PDI-DO** in the memory device.

electrical properties. The energy states of coronene or **PDI-DO** obtained by theoretical calculation or cyclic voltammetry (CV) are illustrated in Figures S11 and S12 of Supporting Information. The HOMO energy levels of **PI(AMTPA)**, coronene, and **PDI-DO** are −5.31, −5.52, and −5.44 eV, respectively, while the LUMO energy levels are −2.23, −1.38, and −3.7 eV, respectively. The high electron affinity of **PDI-DO** coming from its aromatic core and imide groups indicates the strong accepting ability of **PDI-DO**. On the other hand, the low-lying HOMO of coronene with the six peri-fused benzene rings acts as weak donor in this blend system. The stability of conductive charge transfer complexes may depend on the recombination ability of the separated holes/electrons referred to donor−acceptor strength and effective charge delocalization. Basically, the volatile **PI(AMTPA)** device undergoes the charge recombination directly through the back charge transfer in the donor−acceptor covalent connection due to the limited delocalization of **AMTPA** donor and low theoretical dipole moment of basic unit of electrically unstable **PI(AMTPA)**.[9,10] Radical cation and anion of charge transfer complexes are stabilized to form a charge separated state in the presence of coronene within PI blend due to its strong $\pi-\pi$ stacking interaction. As the **PI(AMTPA)**:coronene blend thin film is activated by an electric field, the transferred charged transport and delocalized effectively between two electrodes if much more aromatic coronene weak donors are involved. Therefore, the **PI(AMTPA)**:coronene devices change from the volatile to nonvolatile flash and eventually to WORM behavior in accordance with the coronene content. For the case of **PI(AMTPA)**:**PDI-DO** blend, the stable charge transfer environment can hardly recombine not only due to the close $\pi-\pi$ interaction of hetereocyclic aromatic **PDI-DO** structures but also the high electron affinity of the **PDI-DO** acceptors significantly promote the stronger donor−acceptor interaction. The gradually increasing concentration of **PDI-DO** consecutively leads to an enhanced electrical stability. As delocalized tunneling of field-induced charge transfer carriers occurs through the entire film, the nonvolatile flash/WORM memory behaviors are expected depending on the loading ratio of the **PDI-DO** additives.

The experimental analysis suggests that the switching behavior is highly correlated to the loading ratio of guest additives in polymer host and device with relatively stronger **PDI-DO** acceptors shows more pronounced stability in LRS. Under the prerequisite that the stable charge transfer conductive complex is formed (in other words, nonvolatile behavior is detected), the ability to restrain the back charge transfer is crucial to judge the flash/WORM behaviors. The present **PI(AMTPA)**:3% coronene or 1% **PDI-DO** memory devices exhibit only flash memory effect and the SET/RESET processes can be achieved by negative/positive voltage polarities since difficult charge recombination and back charge transfer occur. This bipolar switching behavior indicates that switching effect has a close relationship on the driven electrical field. However, the nonerasable WORM memory effect in high concentration of coronene (15%) or **PDI-DO** (10%) may arise from irreversible charge transfer migration compared to volatile **PI(AMTPA)** matrix. The switching behaviors follow partially the flash memory and partially the WORM memory if the numbers of additives lie between them. Here, the $V_{th}$(SET) can also be related to the loading ratio of coronene or **PDI-DO** (Figure 11). The electrical features imply that the switching

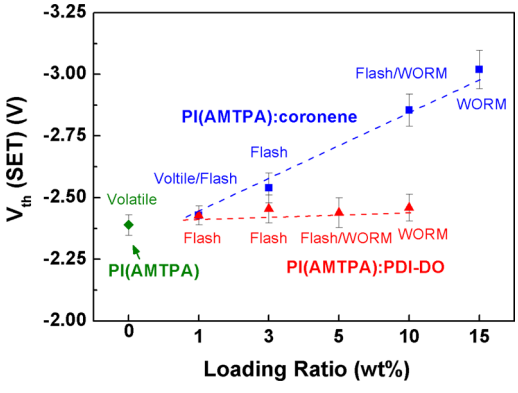


**Figure 11.** Variation on the $V_{th}$(SET) of **PI(AMTPA)**-based memory devices with the loading ratio of coronene or **PDI-DO**.


dx.doi.org/10.1021/am4006594 | ACS Appl. Mater. Interfaces 2013, 5, 4921−4929

may be due to charge polarization along the external electric field effect. As compared to the coronene weak donor, an obvious donor−acceptor interaction between the **PI(AMTPA)** and **PDI-DO** strong acceptor requires a smaller energy for promoting the charge from HOMO of donor to LUMO of acceptor for nonvolatile behavior. Meanwhile, the field enhancement occurs and percolation path is formed with smaller $V_{th}$(SET) attained in all loading ratios of **PI(AMTPA)**:**PDI-DO** blend memory devices. The similarity in $V_{th}$(SET) of **PI(AMTPA)**:**PDI-DO** blend implies that strong donor/acceptor interaction in the hybridization of HOMO/LUMO level has already determined the LRS. On the other hand, the $V_{th}$(SET) in **PI(AMTPA)**:coronene devices depend on loading ratio of additives that basically relies on the differences in the charge injection barriers. Large barriers from deep HOMO of coronene need more external energy to switch the device when the Al electrodes are used. One additional important evidence that can prove the associated strong donor−acceptor interaction between **PI(AMTPA)** and **PDI-DO** acceptor is that the nonvolatile and nonerasable of resistance switching is found with a smaller **PDI-DO** content than coronene. For example, although the 1% **PDI-DO** device becomes flash-type memory and 10% **PDI-DO** device obtains completely WORM memory, it takes 3 and 15% to gain flash and WORM type characteristics, respectively, for the PI/coronene blend.

The present study demonstrates that simple blend materials could provide similar functionalities compared to the corresponding copolymers which requires complex synthetic procedure.[6−11] Both the switching characteristics of **PI(AMTPA)**:coronene or **PDI-DO** change from volatile to nonvolatile flash and WORM as additives increases. The transition between HRS/LRS is erasable flash with the low contents of coronene and **PDI-DO**; in this case, closer interaction of planar additives within the PI matrix can still be done in back charge transfer procedure similar to the blend system, such as reduced graphene oxide[32,33] or hexaazatriphenylene derivatives[35] as guest acceptors. However, more coronene or **PDI-DO** enhances and stabilizes the electrically controlled charge transfer and irreversible WORM memory can be obtained that bears an analogy to the polymer blend with spherical PCBM additives.[21−28]

## CONCLUSIONS

In summary, two-terminal flexible resistor memory devices with a configuration of PEN/Al/**PI(AMTPA)**:coronene or **PDI-DO** blend/Al have been fabricated and characterized. The nonvolatile resistance bistability of PI blend materials based memory devices analyzed using a proper theoretical $J-V$ dependent model is originally attributed to electric field controlled charge transfer and large $\pi-\pi$ conjugated planar backbone. The memory behaviors are varied with the additives contents starting from volatile to nonvolatile flash and WORM memory with an ON/OFF ratio of $\sim 1 \times 0^4$, low operating voltage, long retention time of more than $1 \times 10^4$ s and good endurance even under the various bending conditions. These polymer blend materials provide a viable way to become a memory controller in which a memory device has different types of memory therein (e.g., volatile and nonvolatile flash or WORM) through the loading ratio and relative energy levels of guest additives.

## ASSOCIATED CONTENT

### Supporting Information

FT-IR, $^1$H NMR, and $^{13}$C NMR spectrum of **PDI-DO**. AFM images absorption spectra of PI blend. Additional electrical characteristics, flexibility test and fitted $J-V$ curve of PI blend memory device. Theoretical energy state of coronene. This material is available free of charge via the Internet at http://pubs.acs.org/.

## AUTHOR INFORMATION

### Corresponding Author

*E-mail: chenwc@ntu.edu.tw (W.-C.C.); clliu@ncu.edu.tw (C.-L.L.); ueda.m.ad@m.titech.ac.jp (M.U.).

### Author Contributions

†Authors A.-D.Y, T.K., and Y.-H.C. contributed equally.

### Notes

The authors declare no competing financial interest.

## ACKNOWLEDGMENTS

The financial support from National Science Council (NSC) of Taiwan is highly appreciated. T.K. is thankful for the support from the Japan Society for the Promotion of Science (23·2900).

## REFERENCES

(1) Yang, Y.; Ouyang, J.; Ma, L.; Tseng, R. J. H.; Chu, C. W. *Adv. Funct. Mater.* **2006**, *16*, 1001−1014.
(2) Ling, Q. -D.; Liaw, D. -J.; Zhu, C.; Chan, D. S. -H.; Kang, E. T.; Neoh, K. G. *Prog. Polym. Sci.* **2008**, *33*, 917−978.
(3) Heremans, P.; Gelinck, G. H.; Muller, R. M.; Baeg, K.-J.; Kim, D.-Y.; Noh, Y.-Y. *Chem. Mater.* **2011**, *23*, 341−358.
(4) Liu, C.-L.; Chen, W.-C. *Polym. Chem.* **2011**, *2*, 2169−2174.
(5) Cho, B.; Song, S.; Ji, Y.; Kim, T.-W.; Lee, T. *Adv. Funct. Mater.* **2011**, *21*, 2806−2829.
(6) Fang, Y.-K.; Liu, C.-L.; Li, C.; Lin, C. J.; Mezzenga, R.; Chen, W.-C. *Adv. Funct. Mater.* **2010**, *20*, 3012−3024.
(7) Fang, Y.-K.; Liu, C.-L.; Chen, W.-C. *J. Mater. Chem.* **2011**, *21*, 4778−4786.
(8) Fang, Y.-K.; Liu, C.-L.; Yang, G.-Y.; Chen, P.-C.; Chen, W.-C. *Macromolecules* **2011**, *44*, 2604−2612.
(9) Kurosawa, T.; Lai, Y.-C.; Higashihara, T.; Ueda, M.; Liu, C.-L.; Chen, W.-C. *Macromolecules* **2012**, *45*, 4556−4563.
(10) Yu, A.-D.; Kurosawa, T.; Lai, Y.-C.; Higashihara, T.; Ueda, M.; Chen, W.-C. *J. Mater. Chem.* **2012**, *22*, 20754−20763.
(11) Kurosawa, T.; Lai, Y.-C.; Yu, A.-D.; Wu, H.-C.; Higashihara, T.; Ueda, M.; Chen, W.-C. *J. Polym. Sci., Polym. Chem.* **2013**, *51*, 1348−1358.
(12) Lim, T. W.; Yang, Y.; Li, F.; Kwon, W. L. *NPG Asia Mater.* **2012**, *4*, e18.
(13) Ouyang, J.; Chu, C.-W.; Szmanda, C. R.; Ma, L. P.; Yang, Y. *Nat. Mater.* **2004**, *3*, 918−922.
(14) Tseng, R. J.; Huang, J.; Ouyang, J.; Kaner, R. B.; Yang, Y. *Nano Lett.* **2005**, *5*, 1077−1080.
(15) Baker, C. O.; Shedd, B.; Tseng, R. J.; Martinez-Morales, A. A.; Ozkan, C. S.; Ozkan, M.; Yang, Y.; Kaner, R. B. *ACS Nano* **2011**, *5*, 3469−3474.
(16) De Rosa; Auriemma, C. F.; Di Girolamo, R.; Pepe, G. P.; Napolitano, T.; Scaldaferri, R. *Adv. Mater.* **2010**, *22*, 5414−5419.
(17) Chu, C. W.; Ouyang, J.; Tseng, J.-H.; Yang, Y. *Adv. Mater.* **2005**, *17*, 1440−1443.
(18) Paul, S.; Kanwal, A.; Chhowalla, M. *Nanotechnology* **2006**, *17*, 145−151.
(19) Liu, Z.; Xue, F.; Su, Y.; Varahramyan, K. *IEEE Electron Device Lett.* **2006**, *27*, 151−153.
(20) Song, S.; Cho, B.; Kim, T.-W.; Ji, Y.; Jo, M.; Wang, G.; Choe, M.; Kahng, Y. H.; Hwang, H.; Lee, T. *Adv. Mater.* **2010**, *22*, 5048−5052.

(21) Ji, Y.; Lee, S.; Cho, B.; Song, S.; Lee, T. *ACS Nano* **2011**, *5*, 5995−6000.
(22) Hsu, J.-C.; Liu, C.-L.; Chen, W.-C.; Sugiyama, K.; Hirao, A. *Macromol. Rapid Commun.* **2011**, *32*, 528−533.
(23) Hsu, J.-C.; Chen, Y.; Kakuchi, T.; Chen, W.-C. *Macromolecules* **2011**, *44*, 5168−5177.
(24) Lian, S.-L.; Liu, C.-L.; Chen, W.-C. *ACS Appl. Mater. Interfaces* **2011**, *3*, 4504−4511.
(25) Lai, Y.-C.; Ohshimizu, K.; Lee, W.-Y.; Hsu, J.-C.; Higashihara, T.; Ueda, M.; Chen, W.-C. *J. Mater. Chem.* **2011**, *21*, 14502−14508.
(26) Chen, J.-C.; Liu, C.-L.; Sun, Y.-S.; Tung, S.-H.; Chen, W.-C. *Soft Matter* **2012**, *8*, 526−535.
(27) Liu, J.; Yin, Z.; Cao, X.; Zhao, F.; Lin, A.; Xie, L.; Fan, Q.; Boey, F.; Zhang, H.; Huang, W. *ACS Nano* **2010**, *4*, 3987−3992.
(28) Liu, J.; Lin, Z.; Liu, T.; Yin, Z.; Zhu, X.; Chen, S.; Xie, L.; Boey, F.; Zhang, H.; Huang, W. *Small* **2010**, *6*, 1536−1542.
(29) Liu, G.; Ling, Q.-D.; Teo, E. T. H.; Zhu, C.-X.; D. Chan, S.-H.; Neoh, K.-G.; Kang, E.-T. *ACS Nano* **2009**, *3*, 1929−1937.
(30) Liu, G.; Ling, Q.-D.; Kang, E.-T.; Neoh, K.-G.; Liaw, D.-J.; Chang, F.-C.; Zhu, C.-X.; D. Chan, S.-H. *J. Appl. Phys.* **2007**, *102*, 024502.
(31) Yu, A.-D.; Liu, C.-L.; Chen, W.-C. *Chem. Commun.* **2012**, *48*, 383−385.
(32) Hu, B.; Quhe, R.; Chen, C.; Zhuge, F.; Zhu, X.; Peng, S.; Chen, X.; Pan, L.; Wu, Y.; Zheng, W.; Yan, Q.; Lu, J.; Li, R.-W. *J. Mater. Chem.* **2012**, *22*, 16422−16430.
(33) Wang, S.; Manga, K. K.; Zhao, M.; Bao, Q.; Loh, K. P. *Small* **2011**, *7*, 2372−2378.
(34) Mamo, M. A.; Sustaita, A. O.; Coville, N. J.; Hummelgen, I. V. *Org. Electron.* **2013**, *14*, 175−181.
(35) Sim, R.; Ming, W.; Setiawan, T.; Lee, P. S. *J. Phys. Chem. C* **2013**, *117*, 677−682.
(36) Salaoru, I.; Paul, S. *Thin Solid Films* **2010**, *519*, 559−956.
(37) Suga, T.; Takeuchi, S.; Nishide, H. *Adv. Mater.* **2011**, *23*, 5545−5549.
(38) Park, K. K.; Jung, J. H.; Kim, T. W. *Appl. Phys. Lett.* **2011**, *98*, 193301.
(39) Kurosawa, T.; Higashihara, T.; Ueda, M. *Polym. Chem.* **2013**, *4*, 16−30.
(40) Park, S.; Kim, K.; Kim, D. M.; Kwon, W.; Choi, J.; Ree, M. *ACS Appl. Mater. Interfaces* **2011**, *3*, 765−773.
(41) Ko, Y-.G.; Kwon, W.; Yen, H.-J.; Chang, C.-W.; Kim, D. M.; Kim, K.; Hahm, S. G.; Lee, T. J.; Liou, G. S.; Ree, M. *Macromolecules* **2012**, *45*, 3749−3758.
(42) Hu, B.; Zhuge, F.; Zhu, X.; Peng, S.; Chen, X.; Peng, L.; Yan, Q.; Li, R. W. *J. Mater. Chem.* **2012**, *22*, 520−526.
(43) Zhuge, F.; Hu, B.; He, C.; Zhou, X.; Liu, Z.; Li, R. W. *Carbon* **2011**, *49*, 3796−3802.
(44) Lampert, M. A.; Mark, P. *Current Injection in Solids*; Academic Press: New York, 1970.
(45) Sze, S. M. *Physics of Semiconductor Devices*, 2nd ed.; Wiley: New York, 1998.